Spring 2022

Microbial Community Dynamics During Key Life History Transitions in the Deep-Sea Chemosymbiotic Mussel, Gigantidas childressi

Tessa F. Beaver
Western Washington University, tessabeaver4526@gmail.com

Microbial community dynamics during key life history transitions in the deep-sea chemosymbiotic mussel *Gigantidas childressi*

By

Tessa Francisca Beaver

Accepted in Partial Completion
of the Requirements for the Degree
Master of Science

ADVISORY COMMITTEE

Dr. Shawn M Arellano, Chair

Dr. Heather Fullerton

Dr. Robin Kodner

Dr. Brian Bingham

GRADUATE SCHOOL

David L. Patrick, Dean

Master's Thesis

In presenting this thesis in partial fulfillment of the requirements for a master's degree at Western Washington University, I grant to Western Washington University the non-exclusive royalty-free right to archive, reproduce, distribute, and display the thesis in any and all forms, including electronic format, via any digital library mechanisms maintained by WWU.

I represent and warrant this is my original work, and does not infringe or violate any rights of others. I warrant that I have obtained written permissions from the owner of any third party copyrighted material included in these files.

I acknowledge that I retain ownership rights to the copyright of this work, including but not limited to the right to use all or part of this work in future works, such as articles or books.

Library users are granted permission for individual, research and non-commercial reproduction of this work for educational purposes only. Any further digital posting of this document requires specific permission from the author.

Any copying or publication of this thesis for commercial purposes, or for financial gain, is not allowed without my written permission.

Tessa Francisca Beaver

May 6th, 2022

Microbial community dynamics during key life history transitions in the deep-sea chemosymbiotic mussel *Gigantidas childressi*

A Thesis
Presented to
The Faculty of
Western Washington University

In Partial Fulfillment
Of the Requirements for the Degree
Master of Science

by
Tessa Francisca Beaver
May 2022

Abstract

Marine invertebrates form specific associations with bacterial communities that are different from their environment, change throughout their development, and shape evolutionary and ecological processes. The bathymodiolin (Mytilidae) mussel *Gigantidas childressi* lives at deep-sea methane seeps and relies on methanotrophic endosymbionts for its nutrition. Its larval life, however, is spent feeding in the water column. Upon metamorphosis at a suitable seep habitat, methanotrophic bacteria rapidly colonize gill cells and the juvenile mussel switches to symbiont-derived energy. To determine if the microbiome of the *G. childressi* changes during these transitions, the V3/V4 region of the 16S rRNA gene was sequenced to census the bacterial diversity within *G. childressi* across early development. Like larvae of other deep-sea taxa, diversity was relatively low in all samples, but results show strong evidence for the re-organization of the larval and juvenile microbiomes based on stage-specific shifts in both habitat and nutritional mode. In planktotrophic (feeding) larvae, the microbiome is influenced in part by the environment, with key ASVs assigning to environmental generalists such as *Pseudomonas* and *Sphingomonas*. Other taxa were specific to pediveligers and veligers and were not found in juveniles or the surrounding water. Chloroplast sequences were detected in most swimming larvae, potentially as a component of the larval diet in the form of eukaryotic phytoplankton in the gut. Our results also suggested that initial infection of chemoautotrophic symbionts occur before settlement and metamorphosis in pediveligers of *G. childressi*, which were enriched for several potential chemoautotrophic symbionts that were found in juveniles. In early juveniles, the microbiome is mainly composed of several strains of methanotrophic symbionts known to inhabit *G. childressi*. Unexpectedly, we also detected thiotrophic, sulfur-oxidizing symbionts related to the *SUP05 cluster*, a well-known clade of symbionts in other *Bathymodiolin* species. We also present the first indirect evidence of the heavy-oil degrading *Cycloclasticus* as a symbiont of *G. childressi*. We suspect that the unexpected diversity of symbionts in early juveniles follows a successional pattern where diversity decreases as the mussel grows and matures, eventually resulting in the 1-2 dominate MOX phylotypes commonly observed in adults.

Acknowledgements

I would like to acknowledge the efforts of the crew aboard the R/V Thomas G. Thompson, as well as the teams associated with AUV Sentry and ROV Jason on cruise TN-391. Without their dedication and hard work, none of this would be possible. Additional thanks to members of the Young Lab at the Oregon Institute for Marine Biology: Avery Calhoun, Lauren Rice, and Caitlin Plowman for all their help at sea. I would also like to thank Ahna van Gaest and Dexter Davis for their help and support in the lab. Finally, I would like to acknowledge Dr. Shawn Arellano for mentoring me through the uncertainty of a global pandemic and being an encouraging and supportive advisor.

Table of Contents

List of Tables and Figures

Introduction

In the last decade there has been enormous growth in our understanding of how microbes influence physiology, ecology, and evolution of animal hosts (Wilkins et al. 2019, McFall-Ngai et al. 2015, Kohl & Carey 2016). This has, in large part, been facilitated by technological developments in culture-free methods for examining the diversity of microbial communities in a range of environments (Biteen et al. 2015, McFall-Ngai et al. 2015). New molecular tools have fostered the discovery that host-associated microbial communities are incredibly diverse, essential to life, and functionally tied to more large-scale ecological and evolutionary processes than previously thought (Biteen et al. 2015, McFall-Ngai 2015). There is a growing consensus that host-associated microbial communities are key pieces of the puzzle when trying to predict how an organism will respond to changes in both physiology and environment over its life cycle (Kohl & Carey 2016, McFall-Ngai et al. 2013, McFall-Ngai & Ruby 2000).

A diverse and dynamic microbiome may be a necessary trait for physiological adjustment and development through life-history stages (Kohl & Carey 2016). During development, animals often change their physiology, diet, and habitat across multiple life-stages. These changes can alter the presence and activity of associated microbes, ultimately influencing microbial community structure and function (McFall-Ngai et al. 2015). Thus, animals tend to associate with stage-specific bacterial communities that correlate with changes in morphology and life-history traits (Carrier & Reitzel 2018, Fieth et al. 2016, Mortzfeld et al. 2015, Apprill et al. 2012, Sharp et al. 2012). Microbial partners can also drive the maturation of tissues during key developmental transitions, regardless of the proximity of the tissue to symbiont populations (McFall-Ngai 2014). Moreover, host-associated microbes expand the range of diet supply, shape the immune system, and control pathogenic bacteria in both vertebrates and invertebrates

(McFall-Ngai et al. 2013, Fraune & Bosch 2010). These pieces of evidence all suggest that bacteria play a key and dynamic role in the fitness of a host organism throughout its life cycle, and that host-bacteria interactions should be considered an integral part of development and evolution of host organisms (Mortzfeld et al. 2015).

The complex life cycles of marine invertebrates often involve distinct embryonic, larval, and juvenile and adult stages representing different habitats, nutritional modes, and morphologies (Strathmann 1985, Thorson 1950) that likely necessitate shifts in associated microbiota. Developmental shifts in microbiota have been observed in a range of marine invertebrates with varying levels of influence from the genetics of the host to the environment (Carrier et al. 2020). For example, stage-specific bacterial communities have been observed in the starlet sea anemone, *Nematostella vectensis*, where a clear shift in microbial community composition corresponds to early developmental transitions within the host animal, with little influence from the surrounding environment (Mortzfeld et al. 2015). Conversely, when the free-swimming pelagic larva of the tropical sponge *Amphimedon queenslandica* settles onto the seafloor and metamorphoses into a sessile sponge, a substantial influx of environmentally derived bacteria results in a major reorganization of the microbiome, reducing the abundance of vertically inherited symbionts whose dominance is not restored until adulthood (Fieth et al. 2016).

In chemosynthetic habitats such as hydrothermal vents and cold seeps, many marine invertebrates strictly rely on intracellular, symbiotic bacteria for the bulk of their nutrition (Dubilier et al. 2008). In these partnerships, the animal host supplies symbionts with reduced compounds from the environment, including hydrogen sulfide and methane, as well as oxygen and carbon dioxide needed for their chemosynthetic metabolism (Dubilier et al. 2008, Stewart et

al. 2005) and the symbionts provide their hosts with nutrition (Cavanaugh et al. 2006). Symbionts can be passed directly from parent to offspring (vertically) or acquired from the environment (horizontally) at varying stages of development (Bright & Bulgheresi 2010). These organisms offer a unique system to examine how the host microbiome is affected by metabolic dependence on a particular symbiont, especially in those with complex life-histories and aposymbiotic life stages.

The cold-seep mussel *Gigantidas childressi* (originally *'Bathymodiolus' childressi,* Gustafson et al. 1998) undergoes drastic ontogenetic niche switches that could be associated with re-organization and simplification of the microbiome. *Gigantidas childressi* is a mixotrophic mussel that harbors methane-oxidizing (MOX) endosymbionts in the gills and inhabits cold seeps across a wide depth range of 362m to 2267m (Coykendall et al. 2019, Gustafson et al. 1998). Although *G. childressi* is reliant on symbionts as an adult, the larvae feed while dispersing in the plankton for potentially long durations (3-13 months) (Arellano & Young 2009). While it has been confirmed that larval development is planktotrophic, the specific food sources of *G. childressi* larvae are not known (Arellano et al. 2014, Arellano & Young 2009) but previous work has shown that larvae are capable of vertically migrating hundreds of meters into the photic zone, where they could potentially feed on phytoplankton (Arellano et al. 2014). Thus, the larvae of *G. childressi* may face a wide range of biotic and abiotic conditions during their long pelagic larval duration (Arellano et al. 2014, Arellano & Young 2009). Once a suitable seep habitat is selected, larvae of *G. childressi* face another major habitat and nutritional change as they transition from planktonic pediveligers to benthic, chemosynthetic post-larvae (Franke et al. 2020). Their MOX endosymbionts are most likely acquired from the environment while metamorphosing from settled plantigrade to post-larva, which is when the velum (the larval

feeding and swimming structure) disintegrates, and the adult shell is secreted (Franke et al. 2020). This is the stage at which specific symbionts can initiate contact with the gill epithelium (Franke et al. 2020). Initial establishment of symbiont populations appears to be rapid, as individuals across a narrow developmental range are either fully colonized by their known MOX and SOX (sulfur oxidizing) symbionts or aposymbiotic (symbiont-free) (Franke et al. 2020). Once the ventral groove of the gills is formed, the animal enters the juvenile stage and increases in size and endosymbiont carrying capacity until reaching maturity (Franke et al. 2020, Laming et al. 2018). However, endosymbiont colonization is a continuous process throughout the host's lifetime, and symbionts colonize newly formed gill filaments *de novo* as they grow (Wentrup et al. 2014).

A diverse and dynamic microbiome may be a necessary trait for physiological adjustment through the advancement of these life-history stages (Kohl & Carey 2016, McFall-Ngai et al. 2013, McFall-Ngai & Ruby 2000). While the acquisition of known MOX symbionts has been characterized in bathymodiolins, the microbiomes of these animals remained uninvestigated. This study examined host-associated microbes across a range of early developmental stages corresponding to major life-history transitions in larvae and juveniles of *Gigantidas childressi*. Microbiomes of larval and juvenile mussels were compared across different habitats (deep water column and within a mussel bed) and nutritional modes (planktotrophic and mixotrophic) to look for evidence of either of these transitions in the composition of the associated microbial community. Specifically, we expected *G. childressi* would exhibit stage-specific microbial community shifts before settlement and after symbiont acquisition, with major microbial taxa corresponding to changes in either habitat (microbes from the surrounding water), nutritional mode (evidence of photosynthetic food or potential endosymbionts), or a combination of both.

Methods

Sample Collection – Veligers, pediveligers, and juvenile mussels of *Gigantidas childressi* were collected at Mississippi Canyon 853 at a depth of 1070 meters on June 16th, 2021, using the submersibles ROV *Jason* (Dive J2-1337) and AUV *Sentry* (Dive S595P) (Figure 1, Appendix A, Table 2a). Mississippi Canyon 853 is a well-known hydrocarbon fluid and gas seep mound that contains a structural high above a relatively shallow salt body. This mud volcano is hypothesized to be a site of release for fluid and gas emanating from the Ursa field petroleum basin, which is located just north of the seep site. Carbonate outcroppings and bacterial mats are common here, with small, scattered beds of *G. childressi* and *B. brooksi* mussels (Rowe 2017, Fisher et al. 2007). *Gigantidas childressi* veligers (swimming larvae) were collected in the water column at an altitude of 5 meters above bottom with AUV *Sentry* fitted with the SyPRID sampler (Billings et al. 2016). Juveniles (metamorphosed) and pediveligers (swimming) of *G. childressi* were collected from the interstices of mussel beds with the ROV *Jason* suction sampler and within scoop samples of adults. A paired 2L water sample was also taken at an altitude of 1.5 m at the time of fauna collection with two 4L Niskin bottles equipped on ROV *Jason*. For the purposes of this project, we used these paired water samples as an environmental background sample near the seafloor.

Shipboard Processing - Plankton samples recovered by AUV Sentry were immediately rinsed from the collectors with 0.3 μm filtered seawater into cannisters and placed on ice. Larvae and juveniles recovered from ROV *Jason* suction and scoop samples were rinsed with cold 0.3 μm filtered seawater onto a 253um mesh sieve. Live samples were immediately sorted for *Gigantidas* larvae with dissecting microscopes and were imaged on a compound light

microscope then preserved individually in 0.5 mL centrifuge tubes with 95% molecular grade ethanol. Larvae of G. childressi exhibit variation in settlement size and are known to settle around 400-500um (Arellano and Young 2009). Given that pediveligers and settled post-larvae can be difficult to tell apart by size and external morphology alone, pediveligers were selected by visual confirmation of an identifiable foot and swimming with a velum. Juveniles were selected based on the presence of the yellow juvenile shell and were in a size range of 1-2mm (Figure 1). Samples were stored at -20°C while on the ship.

Water samples were taken just prior to collection of adult mussels with standard 4L Niskin bottles and processed in 2L pairs. Samples were collected into sterilized plastic canisters and stored in cold rooms until processed immediately after recovery. Each sample was transferred onto a 0.2 μm polycarbonate filter using a Millipore filter apparatus and 2L filter flask attached to a portable vacuum pump. Filters were placed into sterile 2mL centrifuge tubes and stored at -80 °C until land-based analysis could be done.

DNA Extraction and Sequencing - DNA was extracted from larval and juvenile mussels at Shannon Point Marine Center in Anacortes, WA using the Nucleospin Tissue XS kit (Machery-Nagel). DNA was extracted from filters using the Fast DNA Spin Kit for Soil (MP Bio). The concentration of DNA was quantified using a Qubit fluorometer (2.0). Library preparation of extracted DNA was carried out following the PCR amplification of the V3-V4 regions of the 16S rRNA gene was carried out using the following primers: Forward: 5' TACGGGNGGCWGCAG, Reverse: 5' GACTACHVGGGTATCTAATCC (S-DBact-0341-b-S-17/S-D-Bact-0785-a-A-2, Klindworth et al. 2013) with Illumina overhang adapters attached. PCR conditions for 16S rRNA amplicons were 95 °C for 3 minutes, with 25 cycles at 95°C for 30 seconds, 55°C for 30 seconds,

and 72°C for 30 seconds, followed by 72°C for 5 minutes and a holding temperature of 4°C. Resulting products were sequenced on an Illumina MiSeq platform using 600 cycle v3 chemistry (Exact Scientific, Ferndale, WA). PCR amplification of the mitochondrial COI barcode region using Bathymodiolin-specific primers (BATH-COI F/R, Heijden et al. 2012) was carried out with the following conditions: 15 minutes at 95°C with 35 cycles of 35s at 94°C, 35s at 48°C, and 70s at 72°C, followed by 7min at 72°C and a final holding temperature of 10°C. Bi-directional Sanger sequencing (Sequetech, Mountain View, CA) of COI PCR products was used to confirm the species of individuals. After processing in Geneious 10.1 (Dotmatics), COI barcode sequences were compared to those in GenBank using the BLAST search and alignment tool.

Bioinformatics – Processing and analysis of Illumina sequences followed the QIIME2 computational pipeline for the V3/V4 region of the 16S rRNA gene by Carrier et al. (2021). Illumina reads with quality information were processed using QIIME 2 (ver. 2021.8; Bolyen et al., 2019). Adapters were removed and forward and reverse reads were paired with VSEARCH (Rognes et al. 2016). Paired sequences were filtered by a minimum quality score of 25 and denoised with Deblur (Amir et al. 2017). Features were analyzed as amplicon sequence variants (ASVs) and were assigned taxonomy using the latest version of the SILVA (ver. 138.1) bacterial database. ASVs that were assigned to Archaea were removed from the analysis. A variance stabilizing transformation (using the R package, DEseq2) was performed on the ASV count data to normalize for differences in library size (McMurdie et al. 2014).

To examine alpha diversity, we tested for differences in the mean numbers of observed ASVs in each group with a non-parametric Kruskal-Wallis test and pairwise Wilcox tests.

Differences in community structure and composition between groups were calculated using unweighted UniFrac distances and compared with hierarchical cluster analysis. A permutational multivariate analysis of variance (PERMANOVA) with pairwise comparisons was used to test for differences in beta-diversity between groups, using a p-value of <0.05 to define significance. Alpha- and beta- diversity plots, taxonomic bar plots, and heatmaps were generated with the R package, Phyloseq (ver. 1.30.0). The QIIME2-based pipeline used to analyze this data is available in Appendix A. The 16S rRNA Illumina reads will be submitted to the Dryad Digital Repository and the Sequence Read Archive database (SRA).

Results

Figure 1 shows representative photos of each of the sample groups examined in this study, all of which were taken on the ship just after collection. Analysis of COI barcodes confirmed that all larval and juvenile samples identified as *Gigantidas childressi* with 99.6-100.0% sequence similarity. Bacterial communities from all 16 *G. childressi* individuals were amplified and sequenced successfully, resulting in a total of 123,841 sequences after processing with processed read counts ranging from 991 to 15,020 per sample (Appendix A, Table 2b). The two highest read counts were both water samples, and there was a much higher concentration of extracted DNA available from the filters compared to the amount of bacterial DNA found in individual larval and juvenile mussels (Appendix A, Table 2b). Despite the lower read counts for mussels, the number of observed ASVs plateaued after approximately 500 reads and rarefaction was achieved for all samples (Figure 2), indicating sufficient sequencing coverage to describe the observed community.

A variance stabilizing transformation (using the R package, DEseq2) was performed on the ASV count data to normalize for differences in library size (McMurdie et al. 2014). This was compared with several other normalization methods: traditional rarefication (subsampling to the smallest library size), scaled-ranked subsampling (SRS), and the centered-log ratio (CLR). The effect of library size on unweighted Unifrac distances was tested with a PERMANOVA for each method, and although library size was a significant factor with all methods, VST (Pseudo-F = 1.65, p = 0.017) introduced the least bias compared to SRS (Pseudo-F = 2.18, p = 0.01), CLR (Pseudo-F = 2.61, p = 0.008), and traditional rarefication (Pseudo-F = 2.33, p = 0.011).

We found a significant effect of group on the mean numbers of ASVs (Figure 3; Kruskal-Wallis, X^2=8.80, p=0.03), but pairwise comparisons between groups were not significantly different (Pairwise Wilcox, p > 0.05). This is likely due to the limits of statistical power from low sample size (n=2) and high variation of niskin samples compared to mussel samples (n = 4-5), even though niskin samples show much higher diversity than the mussels (Figure 2 and 3). On average, veligers associated with 29.25 ± 9.78 bacterial ASVs. Pediveligers associated with more on average but with greater variation (51.8 ± 28.99 ASVs). Juveniles had the second highest average but were also quite variable (65.6 ± 30.39 ASVs), and niskins had the greatest number of ASVs with an average of 369 ± 35.36 ASVs (Figure 3, Appendix A, Table 1b).

Bacterial taxa associated with *G. childressi* individuals also differed based on measures of beta diversity (Figure 4, Table 2). Distances between communities were calculated using unweighted UniFrac values, which consider species presence and absence information and counts the fraction of phylogenetic branch length unique to each community. PERMANOVA (Permutational Multivariate Analysis of Variance) revealed that community structure was significantly different between all groups (Pseudo-F = 2.71, p = 0.001). Results of pairwise tests

are presented in Table 2; the only non-significant pairwise test was between niskins and veligers (Table 2, $p = 0.067$). Hierarchical Cluster Analysis of UniFrac distances between bacterial communities shows that each sample type forms its own cluster, with veligers and pediveligers clustering closer together than juveniles or niskins (Figure 4).

The principal difference between juvenile microbiomes and other groups is the abundance of ASVs related to known chemoautotrophic symbionts belonging to the orders Methylococcales (57-86%), Nitrosococcales (2.7-28.9%), and Thiomicrospirales (2-10.7%) (Figure 5). Dominant taxa in pediveligers and veligers are from the orders Pseudomonadales (32-70%), Sphingomonadales (14-42%), and Burkholderiales (7.4-16.6%) (Figure 5). In water samples, ASVs belonging to Pseudomonadales (15-15.3%) and Oceanospirales (13%) are also abundant, as well as Flavobacteriales (7.7-7.9%) and Sphingomonadales (3.5-3.8%) (Figure 5). Notably, sequences from chloroplasts were also recovered from nearly all pediveligers and veligers (with the exception one veliger) (Figure 5). Two pediveligers and two veligers had <1% of sequences assigned to chloroplasts, the others ranged from 1.8-4.8% (Figure 5).

The top three most abundant ASVs found in juveniles were unassigned Methylomonadaceae (Methylococcales), *Marine Methylotrophic Group 2* (Methylococcales), and Marine Methylotrophic Group 3 (Nitrosococcales) (Figure 6). These ASVs made up 41-74%, 0.5-16%, and 2.7-28.9% of the juvenile microbiome, respectively. Other key ASVs in the juvenile microbiome included members from *Cycloclasticus* (Methylococcales), the *SUP05 cluster* (Thiomicrospirales), and Helicobacteraceae (uncultured Campylobacteriales); which comprised 2.6-10.9%, 2-10.7%, and 0.4-2.5% of sequences in juveniles (Figure 6). Unexpectedly, the abundant ASV from Methylomonadaceae was found in 4 pediveligers (0.2-6.5%) (Figure 6). ASVs from *Cycloclasticus* (0.7-5.7%) and *Marine Methylotrophic Group 2*

(1.3-7.7%) were also detected in 3 pediveligers (Figure 6). None of these chemosymbiotic ASVs were detected in veligers (Figure 6).

In veligers and pediveligers, the most common ASVs were assigned to *Sphingomonas* and *Pseudomonas* (Figure 6). *Pseudomonas* was abundant in niskins (14.9-15.3%), veligers (13.1-33.9%), and pediveligers (6.6-36%) and far less abundant in juveniles (<1% in all samples) (Figure 6). Another ASV belonging to Sphingomonadaceae was specific to niskin samples, while a closely related ASV of the genus *Sphingomonas* was abundant in pediveligers and veligers (9.3-42.3%) and was detected in very low abundance (<1%) in 1 of 2 niskin samples (Figure 6). Another abundant taxon was *Acinetobacter* (Pseudomonadales), which represented between 0.5-4.2% of sequences from veligers and pediveligers (and over 56% in one individual) (Figure 6). One ASV from Oxalobacteraceae (Burkholderiales) was also abundant in swimming larvae, ranging from 2.7-16.6% (Figure 6). Members from *SAR324 clade Marine Group B* (2.1-2.3%), *Sulfurovum* (5-5.7%), and *Alcanivorax* (10.8-11.1%) were unique to niskin samples and were not detected in any mussels (Figure 6).

Two pediveligers were enriched for several ASVs (particularly from *Pseudoalteramonas* and *Pyschrobacter)* that were not detected in any other samples (Figures 5 and 6). These pediveligers harbored different Methylomonadaceae, *Cycloclasticus*, and *Marine Methylotrophic Group* 2 ASVs than the other juveniles and pediveligers (Figure 6).

Discussion

Our findings show that the microbiome of *G. childressi* changes according to transitions in both habitat and nutritional mode during specific stages of development. Like larvae of other deep-sea animals, *G. childressi* exhibits low diversity compared to microbiomes in larvae of

shallow-water species (Carrier et al. 2021). The microbiome of veligers and pediveligers of *G. childressi* shared a few major taxa with the environment, with several others that were unique to larvae and not detected in the water. This suggests some influence of the environment on swimming larvae, but also shows that larvae of *G. childressi* associate with taxa that are not passively obtained from the water. Unexpectedly, we found evidence for acquisition of endosymbionts *before* settlement and metamorphosis in swimming pediveligers, which were presumed to be aposymbiotic based on data from other closely related Bathymodiolin species (Franke et al. 2020). After settlement and metamorphosis, the juvenile microbiome is overwhelmed with ASVs from chemoautotrophic bacteria, including known endosymbionts found in adult *G. childressi* mussels (Coykendall et al. 2019, Gustafson et al. 1998). Notably, there were several other potential endosymbionts in juveniles that have not been described in *G. childressi* but have been observed in closely related species. The acquisition of potential endosymbionts from the environment is a clear driver of microbiome structure and composition in developing juveniles.

Mixed effects of environment and the nutritional mode on microbiomes of swimming larvae

Our results suggested some influence of the environment on the microbiomes of swimming *G. childressi* veliger and pediveliger larvae prior to settlement and metamorphosis and that stochastic or neutral colonization dynamics (Bordenstein & Theis 2015; Sieber et al. 2019) mostly, but not entirely, shape the microbiome during larval stages. If neutral processes explain the microbiomes of *G. childressi* veligers and pediveligers, we would expect their microbiota to resemble that of the surrounding seawater. For example, Carrier et al. (2021) examined the microbiomes of deep-sea larvae from the water column and found that they were

low diversity, compositionally similar across species and samples, and enriched with taxa known to be environmental generalists. Although they did not take environmental samples to compare with the larval microbiomes, Carrier et al. (2021) hypothesized that these bacterial partnerships with deep-sea larvae were formed via neutral processes. In our study, veligers and pediveligers appeared to consistently adopt a subset of generalist taxa from the surrounding water column, but juveniles shared very few taxa with the surrounding water.

The microbiome of larvae is mostly composed of a specific subset of taxa from the surrounding water column, including ASVs from the genus *Pseudomonas* and *Sphingomonas*. Both taxa are known environmental generalists that are widely distributed and have representatives in a variety of habitats, aqueous and terrestrial (Piex et al. 2009, Leyes et al. 2004). One ASV from *Pseudomonas* was particularly abundant in both the near-bottom water and the larval stages, indicating that this genus was likely passively acquired from the immediate surrounding environment. In contrast to *Pseudomonas*, there were two ASVs belonging to family Sphingomonadaceae: one that was abundant in *G. childressi* veligers and pediveligers but represented in low abundance (<1%) in only one of our near seafloor water samples, and one that was abundant in our water samples but was not detected in veligers or most of the pediveligers. Given that *Sphingomonas* is another common environmental generalist, swimming larvae may have acquired a *Sphingomonas* strain from elsewhere in the water column during larval dispersal. Evidence suggests that planktotrophic *G. childressi* veligers can disperse in the plankton for up to over a year and are capable of vertically migrating 100s of meters into the upper water column (Arellano et al. 2014, Arellano & Young 2009). Thus, a near-seafloor water sample may not be a truly representative sample of the environment where larvae spend most of their time developing, or perhaps initially established their microbiomes. It is not known, however, how much time

larvae of *G. childressi* spend at various depths in the water column before settling and metamorphosing. Generalist taxa not found in near-bottom samples, such as *Sphingomonas*, may be passively acquired and established during larval dispersal in a different part of the water-column.

There was some evidence that larval diet may have influenced the enrichment of some taxa within the microbiome of the planktotrophic larval life stages of *G. childressi*. Of the taxa that were unique to veligers and pediveligers, the most abundant were from the family Oxalobacteraceae and the genus *Acinetobacter* (family Moraxellaceae). Members of the family Oxalobacteraceae are common in gut and intestinal microbiomes of various animals, including humans (Kurilshikov et al. 2021), mice (Bian et al. 2017), insects (Latour et al. 2021, Ong et al. 2018), salmon (Wang et al. 2018), manila clams (Milan et al. 2018), and corals (Glasl et al. 2016). *Acinetobacter*, in particular, are enriched in gut microbiomes of both Mediterranean and Baltic blue (Mytilidae) mussels (Uterman et al. 2016, Cavallo et al. 2009). It is unclear what role *Acinetobacter* may play in the *G. childressi* larval microbiome or if it was localized to the *G. childressi* larval gut, but its enrichment in larvae of *G. childressi* when compared to environmental and juvenile samples suggests that it could be important during feeding life-stages where larvae may need to rely more on gut microbiota.

While the specific food sources of *G. childressi* larvae are not yet known, it is suspected that the ability to vertically migrate up to the photic zone may allow larvae to feed on phytoplankton (Arellano et al. 2014). Plastidial sequences are commonly recovered in 16S rRNA amplicon datasets, but these are often discarded as they are typically not of interest to microbiologists (Bennke et al. 2018). We intentionally saved sequences assigned to chloroplasts during analysis to determine if there is any evidence of photosynthetic food in the gut. Sequences

assigning to chloroplasts (likely from a photosynthetic eukaryote) were detected in 3 pediveligers and 2 veligers. The relative abundance of chloroplast DNA was low (1-5%) and neither ASV was detected in the surrounding water. The lack of chloroplast DNA in the near-seafloor sample indicates that larvae may have acquired these sequences by vertically migrating to upper water column to feed on phytoplankton. We hypothesize these sequences could represent a component of the larval diet, but further investigation would be needed to confirm this observation. Furthermore, whole-body amplicon sequencing of planktonic individuals may be a promising avenue for future research into understanding the diets of deep-sea larvae, which has largely remained a black box (Young et al. 2017).

Acquisition of chemoautotrophic symbionts drives structure and composition of microbiome

While several species of Bathymodiolin mussels are known to support multiple functionally diverse symbioses (Ansorge et al. 2019, Franke et al. 2020, Duperron et al. 2009), *G. childressi* is known to only house MOX symbionts, with one predominant MOX symbiont phylotype and only 1 or 2 other MOX phylotypes present at most (Franke et al. 2020, Somoza et al. 2021, Coykendall et al. 2019, Duperron et al. 2009). Using whole-body amplicon sequencing, in 4 of 5 *G. childressi* pediveligers we detected several potential MOX symbiont ASVs including those assigned to Methylomonadaceae, Marine Methylotrophic Group 2 (MMG 2), as well as other chemoautotrophic groups like *Cycloclasticus* and sulfur oxidizing Campylobacterota. Although it is not possible to confirm if they are true intracellular endosymbionts localized to gill tissue with our method, the high relative abundance compared to fully aposymbiotic veligers and the surrounding seawater suggests that their detection is unlikely to be contamination.

In *G. childressi* juveniles, the microbiome was mainly composed of several strains of methanotrophic bacteria known as endosymbionts in *G. childressi*, including those assigned to Methylomonadaceae, MMG 2 and Marine Methylotrophic Group 3 (MMG 3). These well-characterized taxa are likely to be intracellular and localized within the gills as they are known to be present in this species at this life-stage (Somoza et al. 2021, Franke et al. 2020, Coykendall et al. 2019). Unexpectedly, thiotrophic taxa were also detected in our small juveniles as well. While they were not abundant in this dataset compared to the methanotrophic taxa, the consistent detection of sulfur oxidizing Campylobacterota in all five juvenile samples supports the hypothesis that *G. childressi* could be capable of relying on thiotrophy to some extent (Coykendall et al. 2019, Assie et al. 2016). Assie et al. (2016) discovered a widespread association between *Bathymodiolus* mussels and an epibiotic Campylobacterota that is closely related to sulfur oxidizers from the Thiovulgaceae family. This epibiotic strain was particularly abundant in *G. childressi* and was found attached to the surface of the gills, a likely advantageous location for acquiring hydrogen sulfide from the water (Assie et al. 2016). Coykendall et al. (2019) found further evidence of thiotrophy in *G. childressi* when a similar phylotype was found in a notable fraction of adult gill samples from the Baltimore and Norfolk Canyon seep sites in the Western Atlantic. ASVs from the thiotrophic SUP05 Clade were also represented in all five juvenile mussels**.** Species belonging to the SUP05 clade are sulfur-oxidizing (SOX) gamma- proteobacteria that exist as both free-living bacteria and intracellular symbionts in several *Bathymodiolin* mussels (*B. azoricus, B. puteoserpentis, B. heckerae)* at both hydrothermal vents and cold seeps (Zhou et al. 2019).

Interestingly, *Cycloclasticus*, a genus known for degrading polycyclic aromatic hydrocarbons (PAHs), was also abundant in our pediveligers and early juveniles—in some cases,

just as prevalently as ASVs from MMG 2 and 3. *Cycloclasticus* is known to metabolize isotopically heavy aromatic hydrocarbons and is often found in association with oil spills and marine sediments (Raggi et al. 2017). This genus has been recently characterized as an endosymbiont in a closely related species of mussel, *Bathymodiolus heckerae,* and in sponges at nearby sites, but has never been described in *G. childressi* (Arellano et al. 2012, Raggi et al. 2013, Rubin-Blum et al. 2017). Our study site is characterized as a mud volcano with high concentrations of methane, and crude oil is not a particularly abundant resource here (Rowe 2017). We suggest that a comparison to oil-dominated seeps, like those studied in Raggi et al (2013) and Rubin-Blum et al. (2017), may be a promising opportunity for studying the retention of this symbiont in *Bathymodiolin* mussels.

It should be noted that we detected the potential parasite *Candidatus endonucleobacter* in all five juveniles and two pediveligers. This bacterium is a known intranuclear parasite of at least 7 species of *Bathymodiolin* mussels and is known as *Candidatus endonucleobacter bathymodioli* (Zielinksi et al. 2009). This bacterium most heavily colonizes symbiont-free cells in gill tissue but was also found in nuclei of the gut, digestive gland, labial palp, mantle, and foot (Zielinksi et al. 2009). We show here that this parasite is found in *G. childressi* during early developmental stages, and may potentially be colonizing in tandem with chemoautotrophic symbionts as suggested by the presence of the bacterium only in pediveligers and juveniles containing symbiont ASVs.

We show here that initial infection of chemoautotrophic symbionts may occur *before* settlement and metamorphosis in pediveligers of *G. childressi*, which is earlier than was previously assumed for this species. Previous evidence supported that Bathymodiolin mussels acquire chemoautotrophic symbionts from the environment *after* settlement and metamorphosis

(Franke et al. 2020). However, the exact timing of symbiont acquisition has only been investigated in one Bathymodiolin species, *Bathymodiolus puteoserpentis* (Franke et al. 2020). Franke et al. (2020) carried out whole-body fluorescent in-situ hybridization (FISH) using specific probes for specific known MOX and SOX endosymbionts to determine when and where these symbionts colonize the vent mussel *B. puteoserpentis*. They found that pediveligers were completely aposymbiotic in all parts of the body (Franke et al. 2020). Using whole-body amplicon sequencing, our data suggests that pediveligers and small juveniles (< 2mm) of *G. childressi* are initially colonized by a diverse suite of chemoautotrophic bacteria. A similar whole-body FISH study has not been carried for *G. childressi* and specific patterns of symbiont colonization may vary by host species. Further investigation across a wider span of life stages is needed to determine if the chemoautotrophic taxa we identified in the microbiome of pediveligers, and early juveniles are true endosymbionts and if symbiotic diversity decreases with age post-acquisition.

We hypothesize that the unexpected diversity of chemoautotrophic symbionts beginning in pediveligers and persisting in small juveniles follows a successional pattern that diminishes in variety as MOX symbionts are selected for by the host and/or environment over time. In *B. puteoserpentis*, colonization by specific MOX and SOX endosymbionts is initiated when the larval feeding structure (velum) degrades, and the infection occurs in other parts of the body before proceeding to gill tissue in plantigrades (Franke et al. 2020). However, it is hypothesized that the ability to host multiple symbiont types is common in symbioses where the environment, rather than the host, fuels the symbionts (Ansorge et al. 2019). Similarly, Ucker et al. (2021) found that geography, rather than host species, explained symbiont genetic variability in *Bathymodiolus* mussels and suggested that the availability of free-living symbionts in the

environment is a key driver of symbiont function and diversity. Given that *G. childressi* obtains symbionts via the environment, initial colonization by many types of bacteria may be possible, with the concentration of various source chemicals in the surrounding water driving bacterial competition and succession within the environment and gill tissue as the juvenile continues to grow and develop. Finally, the early indiscriminate acquisition of chemosymbiotic bacteria beginning as pediveligers, could be a cue for settlement or signal metamorphosis in the right habitat for these endemic cold-seep mussels (Franke et al. 2020, Arellano & Young 2010, McFall-Nai et al. 2013, Hadfield 2011, Song et al. 2020, Friere et al. 2019).

Figure 1. Images of the three developmental stages of *Gigantidas* investigated in this study, taken on a compound light microscope on the 4x objective at 40x total magnification. Top left: A veliger found 5 meters above the bottom with SyPRID. Approx. 500um. Top right: A pediveliger with a visible foot and a velum, but no juvenile shell collected from the seafloor. Bottom: A juvenile with the large, clear juvenile shell present and many gill slits, also collected from the seafloor.

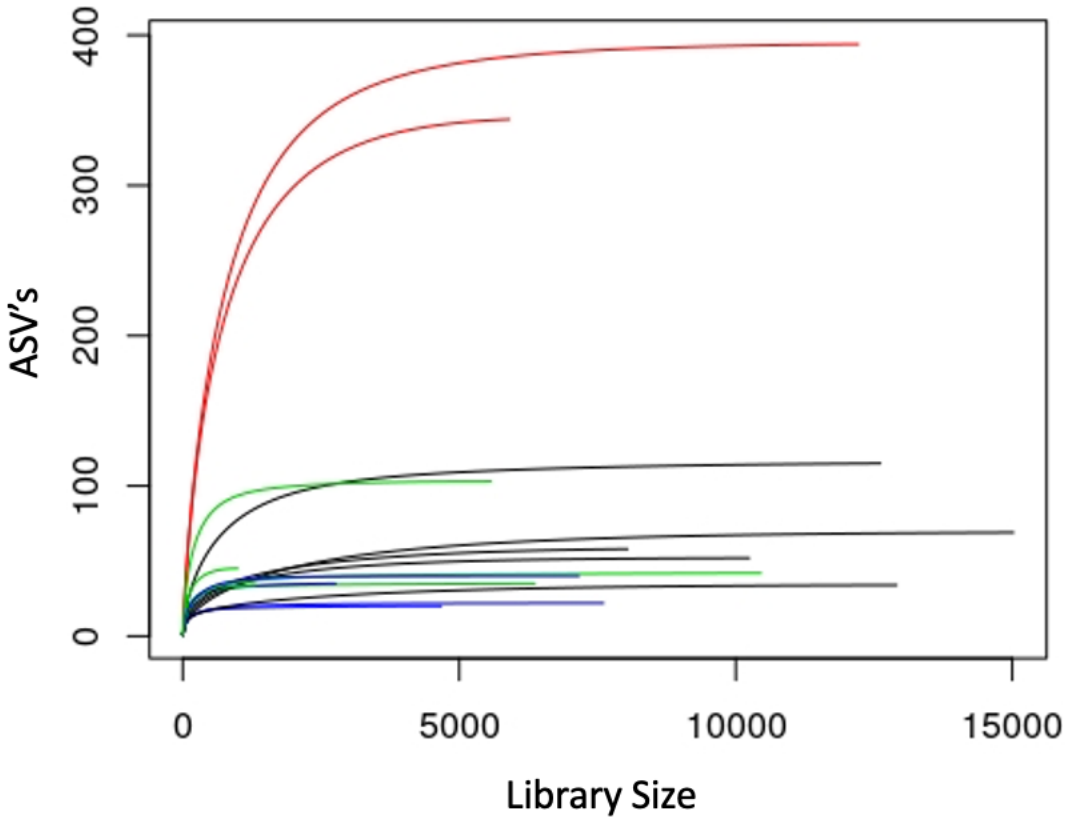

Figure 2. Rarefaction curves of V3-V4 16S rRNA bacterial DNA sequences for 16 samples with veligers (blue), pediveligers (green), juveniles (black) and water samples (red). The # of ASVs is presented as a function of sample size, with plateaus indicating that sufficient sequencing has been done to represent the entire bacterial community. The smallest library size was 991 reads.

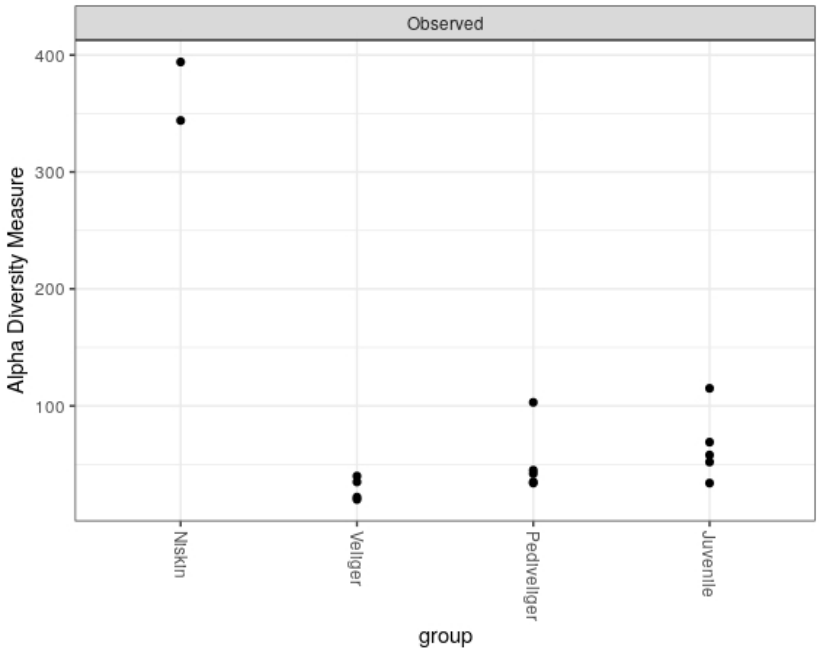

Figure 3. Strip plot of the number of observed ASVs in each sample, organized by group. There was a significant effect of group on the mean numbers of ASVs (Kruskal-Wallis, C^2=8.797, p=0.032).

Table 1. Results of the PERMANOVA and pairwise tests performed on each group of samples to test for differences in beta-diversity. Sample size, pseudo-F values, and p-values are also shown with asterisks to indicate significance level.

Group 1	***Group 2***	***Sample size***	***pseudo-F***	***p-value***
All		16	2.7093	0.001***
Juvenile	Niskin	7	4.9227	0.049*
Juvenile	Pediveliger	10	2.9894	0.009**
Juvenile	Veliger	9	2.8431	0.014*
Niskin	Pediveliger	7	2.8152	0.05*
Niskin	Veliger	6	2.7168	0.067
Pediveliger	Veliger	9	1.4038	0.007**

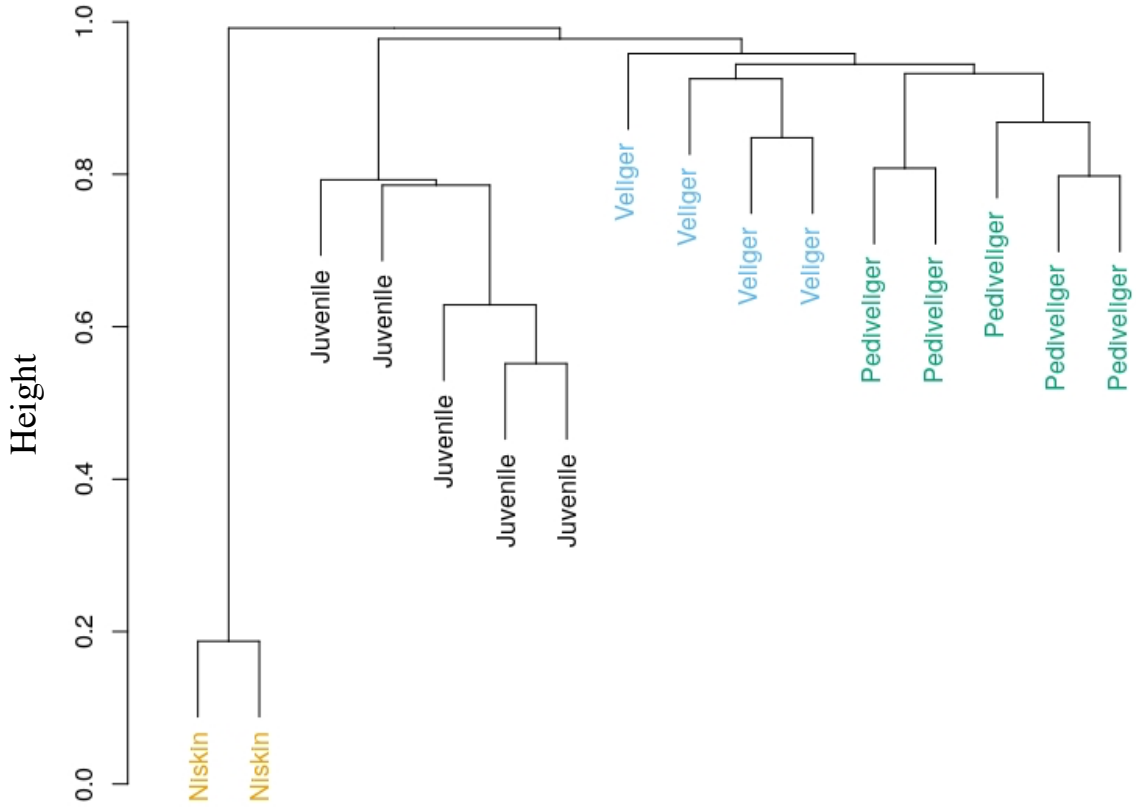

Figure 4. Hierarchical cluster analysis using unweighted UniFrac distances to compare beta-diversity between the bacterial communities of each sample.

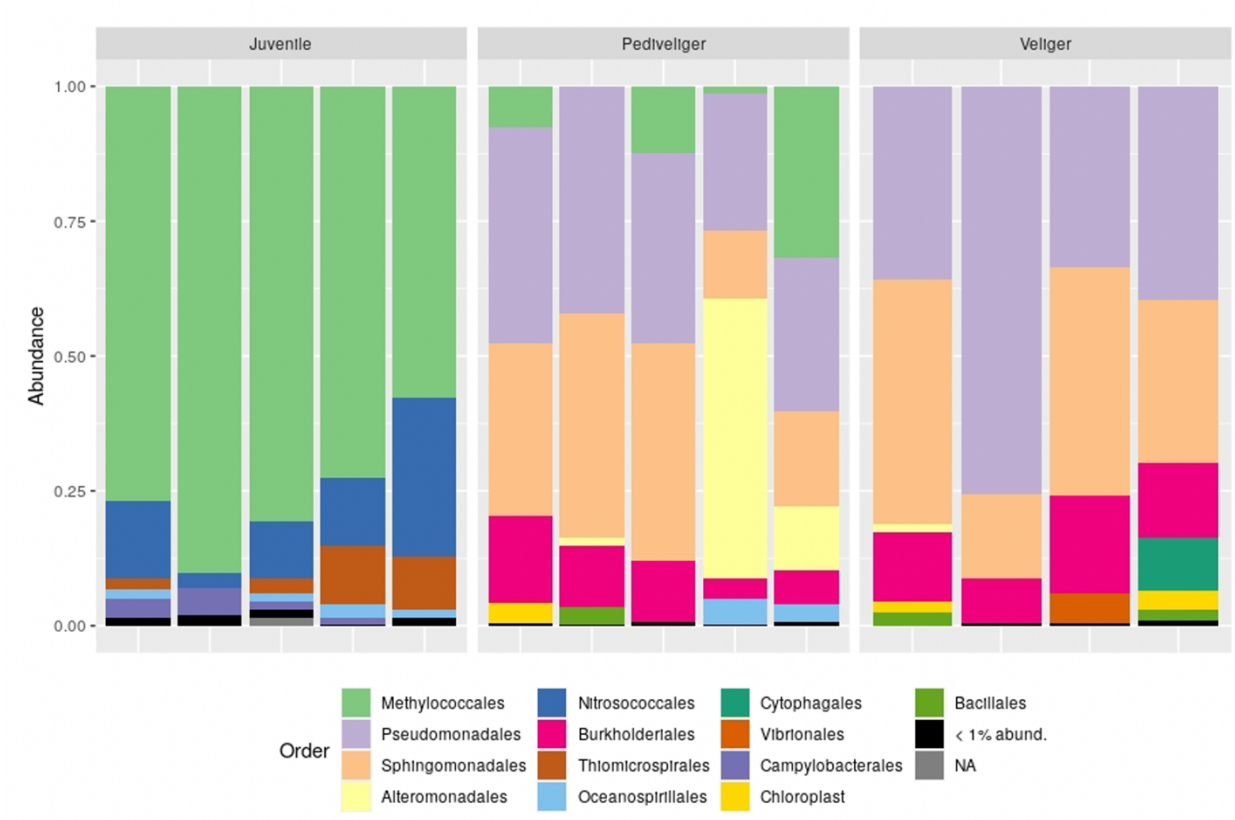

Figure 5. Relative abundance (0-1) of bacterial orders from the top 50 most abundant ASVs in the dataset, with each individual normalized to 1. Each bar represents an individual sample, as indicated on the x axis.

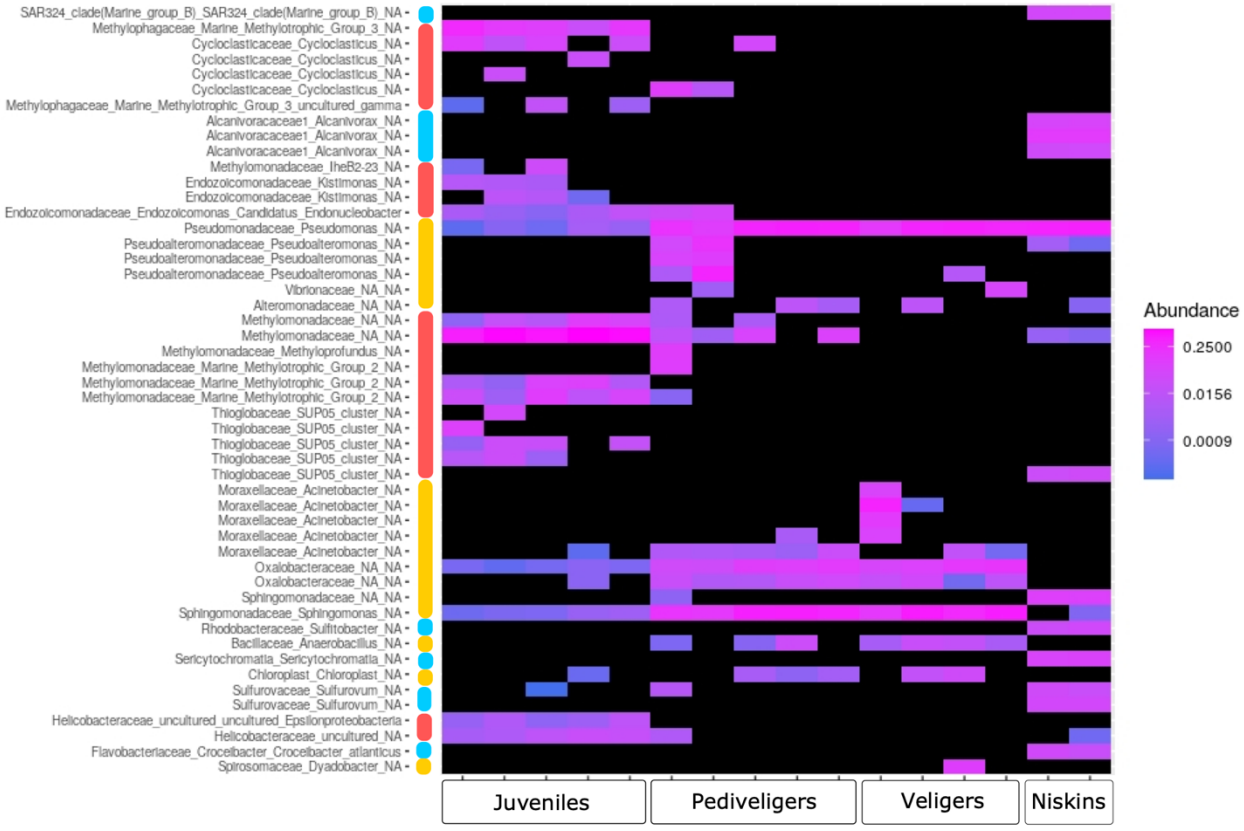

Figure 6. Heatmap of the relative abundance (0-1) of the top 50 ASVs in the dataset, with each individual normalized to 1. Each row represents a unique ASV with family, genus, and species-level taxonomy indicated on the left. Unresolved taxonomic levels are represented with an NA value. Colored bars on the left indicate key groups of bacterial taxa enriched in juveniles (red), pediveligers and veligers (yellow), and niskins (blue).

Work Cited

Aldred, N., & Nelson, A. (2019). Microbiome acquisition during larval settlement of the barnacle *Semibalanus balanoides.* Biology Letters, 15(6), 20180763. doi:10.1098/rsbl.2018.0763

Amir, A., McDonald, D., Navas-Molina, J. A., Kopylova, E., Morton, J. T., Xu, Z. Z., … Knight, R. (2017). Deblur Rapidly Resolves Single-Nucleotide Community Sequence Patterns. *MSystems*, *2*(2), e00191-16. doi:10.1128/msystems.00191-16

Ansorge, R., Romano, S., Sayavedra, L., Porras, M. Á. G., Kupczok, A., Tegetmeyer, H. E., … Petersen, J. (2019). Functional diversity enables multiple symbiont strains to coexist in deep-sea mussels. *Nature Microbiology*, *4*(12), 2487–2497. doi:10.1038/s41564-019-0572-9

Apprill, A. (2019). The Role of Symbioses in the Adaptation and Stress Responses of Marine Organisms. Annual Review of Marine Science, 12(1), 1–24. doi:10.1146/annurev-marine-010419-010641

Arellano, S. M., Gaest, A. L. V., Johnson, S. B., Vrijenhoek, R. C., & Young, C. M. (2014). Larvae from deep-sea methane seeps disperse in surface waters. Proceedings of the Royal Society B: Biological Sciences, 281(1786), 20133276–20133276.

Assié, A., Borowski, C., Heijden, K. van der, Raggi, L., Geier, B., Leisch, N., … Petersen, J. M. (2016). A specific and widespread association between deep-sea Bathymodiolus mussels and a novel family of Epsilonproteobacteria. *Environmental Microbiology Reports*, *8*(5), 805–813. doi:10.1111/1758-2229.12442

Arellano, S. M., & Young, C. M. (2009). Spawning, development, and the duration of larval life in a deep-sea cold-seep mussel. The Biological Bulletin, 216(2), 149–162. doi:10.1086/bblv216n2p149

Arellano, S. & Young, C. Pre- and post-settlement factors controlling spatial variation in recruitment across a cold-seep mussel bed. Marine Ecology Progress Series, 414, 131–144 (2010).

Beinart, R. A., Sanders, J. G., Faure, B., Sylva, S. P., Lee, R. W., Becker, E. L., Gartman, A., Luther, G. W., Seewald, J. S., Fisher, C. R., & Girguis, P. R. (2012). Evidence for the role of endosymbionts in regional-scale habitat partitioning by hydrothermal vent symbioses. Proceedings of the National Academy of Sciences, 109(47), E3241–E3250.

Bennke, C. M., Pollehne, F., Müller, A., Hansen, R., Kreikemeyer, B., & Labrenz, M. (2018). The distribution of phytoplankton in the Baltic Sea assessed by a prokaryotic 16S rRNA gene primer system. Journal of Plankton Research, 40(3), 244–254. doi:10.1093/plankt/fby008

Bian, X., Chi, L., Gao, B., Tu, P., Ru, H., & Lu, K. (2017). The artificial sweetener acesulfame potassium affects the gut microbiome and body weight gain in CD-1 mice. *PLoS ONE*, *12*(6), e0178426. doi:10.1371/journal.pone.0178426

Billings, A., Kaiser, C., Young, C. M., Hiebert, L. S., Cole, E., Wagner, J. K. S., & Dover, C. L. V. (2017). SyPRID sampler: A large-volume, high-resolution, autonomous, deep-ocean precision plankton sampling system. Deep Sea Research Part II: Topical Studies in Oceanography, 137, 297–306. doi:10.1016/j.dsr2.2016.05.007

Biteen, J. S., Blainey, P. C., Cardon, Z. G., Chun, M., Church, G. M., Dorrestein, P. C., … Young, T. D. (2016). Tools for the Microbiome: Nano and Beyond. ACS Nano, 10(1), 6–37. doi:10.1021/acsnano.5b07826

Bolyen, E., Rideout, J. R., Dillon, M. R., Bokulich, N. A., Abnet, C. C., Al-Ghalith, G. A., … Caporaso, J. G. (2019). Reproducible, interactive, scalable and extensible microbiome data science using QIIME 2. *Nature Biotechnology*, *37*(8), 852–857. doi:10.1038/s41587-019-0209-9

Bordenstein, S. R., & Theis, K. R. (2015). Host Biology in Light of the Microbiome: Ten Principles of Holobionts and Hologenomes. *PLOS Biology*, *13*(8), e1002226. doi:10.1371/journal.pbio.1002226

Bright, M., & Bulgheresi, S. (2010). A complex journey: transmission of microbial symbionts. Nature reviews. Microbiology, 8(3), 218–230. https://doi.org/10.1038/nrmicro2262

Cavallo, R. A., Acquaviva, M. I., & Stabili, L. (2009). Culturable heterotrophic bacteria in seawater and Mytilus galloprovincialis from a Mediterranean area (Northern Ionian Sea – Italy). *Environmental Monitoring and Assessment*, *149*(1–4), 465–475. doi:10.1007/s10661-008-0223-8

Cavanaugh, C. M., McKiness, Z. P., Newton, I. L., & Stewart, F. J. (2006). Marine chemosynthetic symbioses. The prokaryotes, 1, 475-507.

Carrier, T. J., Lessios, H. A., & Reitzel, A. M. (2020). Divergent microbiota of echinoid eggs separated by the Isthmus of Panama. BioRxiv, 2020.03.30.015578. doi:10.1101/2020.03.30.015578

Carrier, T. J., Dupont, S., & Reitzel, A. M. (2019). Geographic location and food availability offer differing levels of influence on the bacterial communities associated with larval sea urchins. FEMS Microbiology Ecology, 95(8). doi:10.1093/femsec/fiz103

Carrier, T. J., & Reitzel, A. M. (2018). Convergent shifts in host-associated microbial communities across environmentally elicited phenotypes. Nature Communications, 9(1), 952. doi:10.1038/s41467-018-03383-w

Cordes, E. E., Bergquist, D. C., & Fisher, C. R. (2009). Macro-Ecology of Gulf of Mexico Cold Seeps. Annual Review of Marine Science, 1(1), 143–168. doi:10.1146/annurev.marine.010908.163912

Coykendall, D. K., Cornman, R. S., Prouty, N. G., Brooke, S., Demopoulos, A. W. J., & Morrison, C. L. (2019). Molecular characterization of Bathymodiolus mussels and gill symbionts associated with chemosynthetic habitats from the U.S. Atlantic margin. PLOS ONE, 14(3), e0211616. doi:10.1371/journal.pone.0211616

David, L. A., Maurice, C. F., Carmody, R. N., Gootenberg, D. B., Button, J. E., Wolfe, B. E., … Turnbaugh, P. J. (2014). Diet rapidly and reproducibly alters the human gut microbiome. Nature, 505(7484), 559–563. doi:10.1038/nature12820

Decelle, J., Romac, S., Stern, R. F., Bendif, E. M., Zingone, A., Audic, S., … Christen, R. (2015). PhytoREF: a reference database of the plastidial 16S rRNA gene of photosynthetic eukaryotes with curated taxonomy. Molecular Ecology Resources, 15(6), 1435–1445. doi:10.1111/1755-0998.12401

Demopoulos, A., McClain-Counts, J., Bourque, Jill., Prouty, N., Smith, B., Brooke, S., Ross, S., & Ruppel, C. (2019). Examination of Bathymodiolus childressi nutritional sources, isotopic niches, and food-web linkages at two seeps in the US Atlantic margin using stable isotope analysis and

mixing models. Deep Sea Research Part I: Oceanographic Research Papers. 148. 10.1016/j.dsr.2019.04.002.

Dubilier, N. & Bergin, C. & Lott, C. (2008). Symbiotic diversity in marine animals: the art of harnessing chemosynthesis. Nat Rev Micro 6: 725-740. Nature reviews. Microbiology. 6. 725-40. 10.1038/nrmicro1992.

Duperron, S., Lorion, J., Samadi, S., Gros, O., & Gaill, F. (2009). Symbioses between deep-sea mussels (Mytilidae: Bathymodiolinae) and chemosynthetic bacteria: diversity, function and evolution. *Comptes Rendus Biologies*, *332*(2–3), 298–310. doi:10.1016/j.crvi.2008.08.003

Fieth, R. A., Gauthier, M.-E. A., Bayes, J., Green, K. M., & Degnan, S. M. (2016). Ontogenetic Changes in the Bacterial Symbiont Community of the Tropical Demosponge Amphimedon queenslandica: Metamorphosis Is a New Beginning. Frontiers in Marine Science, 3, 228. doi:10.3389/fmars.2016.00228

Fisher, C. R., Childress, J. J., Oremland, R. S., & Bidigare, R. R. (1987). The importance of methane and thiosulfate in the metabolism of the bacterial symbionts of two deep-sea mussels. Marine Biology, 96(1), 59–71. doi:10.1007/bf00394838

Fisher, C., Roberts, H., Cordes, E., & Bernard, B. (2007). Cold Seeps and Associated Communities of the Gulf of Mexico. Oceanography, 20(4), 118–129. doi:10.5670/oceanog.2007.12

Folmer, O., Black, M., Hoeh, W., Lutz, R., & Vrijenhoek, R. (1994). DNA primers for amplification of mitochondrial Cytochrome C oxidase subunit I from diverse metazoan invertebrates. Molecular Marine Biology and Biotechnology, 5(3), 294–299.

Franke, M., Geier, B., Hammel, J. U., Dubilier, N., & Leisch, N. (2020). Becoming symbiotic – the symbiont acquisition and the early development of bathymodiolin mussels. BioRxiv, 2020.10.09.333211. doi:10.1101/2020.10.09.333211

Fraune, S., & Bosch, T. C. G. (2010). Why bacteria matter in animal development and evolution. *BioEssays*, *32*(7), 571–580. doi:10.1002/bies.200900192

Freire, I., Gutner-Hoch, E., Muras, A., Benayahu, Y., & Otero, A. (2019). The effect of bacteria on planula-larvae settlement and metamorphosis in the octocoral Rhytisma fulvum fulvum. PLoS ONE, 14(9), e0223214. doi:10.1371/journal.pone.0223214

Glasl, B., Herndl, G. J., & Frade, P. R. (2016). The microbiome of coral surface mucus has a key role in mediating holobiont health and survival upon disturbance. The ISME Journal, 10(9), 2280–2292. doi:10.1038/ismej.2016.9

Gustafson, R. G., Turner, R. D., Lutz, R., & Vrijenhoek, R. C. (1998). A new genus and five new species of mussels (Bivalvia, Mytilidae) from deep-sea sulfide/hydrocarbon seeps in the Gulf of Mexico. Malacologia, 40(1-2), 63-112.

Hadfield, M. G. (2011). Biofilms and Marine Invertebrate Larvae: What Bacteria Produce That Larvae Use to Choose Settlement Sites. Annual Review of Marine Science, 3(1), 453–470. doi:10.1146/annurev-marine-120709-142753

Hadfield, M. G. & Paul, V. (2001). Natural Chemical Cues for Settlement and Metamorphosis of Marine-Invertebrate Larvae. Marine Chemical Ecology. 10.1201/9781420036602.ch13.

Hebert, P. D. N., Cywinska, A., Ball, S. L., & deWaard, J. R. (2003). Biological identifications through DNA barcodes. Proceedings of the Royal Society of London. Series B: Biological Sciences, 270(1512), 313–321.

Hiebert, T. C., & Maslakova, S. (2015). Integrative Taxonomy of the Micrura alaskensis Coe, 1901 Species Complex (Nemertea: Heteronemertea), with Descriptions of a New Genus Maculaura gen. nov. and Four New Species from the NE Pacific. *Zoological Science*, *32*(6), 615–637. doi:10.2108/zs150011

Klindworth, A., Pruesse, E., Schweer, T., Peplies, J., Quast, C., Horn, M., & Glöckner, F. O. (2013). Evaluation of general 16S ribosomal RNA gene PCR primers for classical and next-generation sequencing-based diversity studies. Nucleic Acids Research, 41(1), e1–e1. doi:10.1093/nar/gks808

Kohl, K. D., & Carey, H. V. (2016). A place for host–microbe symbiosis in the comparative physiologist's toolbox. Journal of Experimental Biology, 219(22), 3496–3504. doi:10.1242/jeb.136325

Kozich, J. J., Westcott, S. L., Baxter, N. T., Highlander, S. K., & Schloss, P. D. (2013). Development of a Dual-Index Sequencing Strategy and Curation Pipeline for Analyzing Amplicon Sequence Data on the MiSeq Illumina Sequencing Platform. Applied and Environmental Microbiology, 79(17), 5112–5120. doi:10.1128/aem.01043-13

Kurilshikov, A., Medina-Gomez, C., Bacigalupe, R., Radjabzadeh, D., Wang, J., Demirkan, A., … Zhernakova, A. (2021). Large-scale association analyses identify host factors influencing human gut microbiome composition. Nature Genetics, 53(2), 156–165. doi:10.1038/s41588-020-00763-1

Laming, S. R., Gaudron, S. M., & Duperron, S. (2018). Lifecycle Ecology of Deep-Sea Chemosymbiotic Mussels: A Review. Frontiers in Marine Science, 5, 282. doi:10.3389/fmars.2018.00282

Latour, S., Noël, G., Serteyn, L., Sare, A. R., Massart, S., Delvigne, F., & Francis, F. (2021). Multi-omics approach reveals new insights into the gut microbiome of Galleria mellonella (Lepidoptera:Pyralidae) exposed to polyethylene diet. *BioRxiv*, 2021.06.04.446152. doi:10.1101/2021.06.04.446152

McFall-Ngai, M. J. (2015). Giving microbes their due – animal life in a microbially dominant world. The Journal of Experimental Biology, 218(12), 1968–1973. doi:10.1242/jeb.115121

McFall-Ngai, M. J. (2014). The Importance of Microbes in Animal Development: Lessons from the Squid-Vibrio Symbiosis. *Annual Review of Microbiology*, *68*(1), 1–18. doi:10.1146/annurev-micro-091313-103654

McFall-Ngai, M. J., & Ruby, E. G. (2000). Developmental biology in marine invertebrate symbioses. Current Opinion in Microbiology, 3(6), 603–607. doi:10.1016/s1369-5274(00)00147-8

McFall-Ngai, M., Hadfield, M. G., Bosch, T. C. G., Carey, H. V., Domazet-Lošo, T., Douglas, A. E., … Wernegreen, J. J. (2013). Animals in a bacterial world, a new imperative for the life sciences. Proceedings of the National Academy of Sciences, 110(9), 3229–3236. doi:10.1073/pnas.1218525110

Milan, M., Carraro, L., Fariselli, P., Martino, M. E., Cavalieri, D., Vitali, F., … Cardazzo, B. (2018). Microbiota and environmental stress: how pollution affects microbial communities in Manila clams. Aquatic Toxicology, 194, 195–207. doi:10.1016/j.aquatox.2017.11.019

Mortzfeld, B. M., Urbanski, S., Reitzel, A. M., Künzel, S., Technau, U., & Fraune, S. (2016). Response of bacterial colonization in Nematostella vectensis to development, environment and biogeography. Environmental Microbiology, 18(6), 1764–1781. doi:10.1111/1462-2920.12926

Ong, S. Y., Kho, H.-P., Riedel, S. L., Kim, S.-W., Gan, C.-Y., Taylor, T. D., & Sudesh, K. (2018). An integrative study on biologically recovered polyhydroxyalkanoates (PHAs) and simultaneous assessment of gut microbiome in yellow mealworm. Journal of Biotechnology, 265, 31–39. doi:10.1016/j.jbiotec.2017.10.017

Peix, A., Ramírez-Bahena, M.-H., & Velázquez, E. (2009). Historical evolution and current status of the taxonomy of genus Pseudomonas. *Infection, Genetics and Evolution*, *9*(6), 1132–1147. doi:10.1016/j.meegid.2009.08.001

Raggi, L., Schubotz, F., Hinrichs, K. -U., Dubilier, N., & Petersen, J. M. (2013). Bacterial symbionts of Bathymodiolus mussels and Escarpia tubeworms from Chapopote, an asphalt seep in the southern Gulf of Mexico. Environmental Microbiology, 15(7), 1969–1987. doi:10.1111/1462-2920.12051

Rognes, T., Flouri, T., Nichols, B., Quince, C., & Mahé, F. (2016). VSEARCH: a versatile open source tool for metagenomics. *PeerJ*, *4*, e2584. doi:10.7717/peerj.2584

Rubin-Blum, M., Antony, C. P., Borowski, C., Sayavedra, L., Pape, T., Sahling, H., … Dubilier, N. (2017). Short-chain alkanes fuel mussel and sponge Cycloclasticus symbionts from deep-sea gas and oil seeps. Nature Microbiology, 2(8), 17093. doi:10.1038/nmicrobiol.2017.93

Sharp, K. H., Distel, D., & Paul, V. J. (2012). Diversity and dynamics of bacterial communities in early life stages of the Caribbean coral Porites astreoides. *The ISME Journal*, *6*(4), 790–801. doi:10.1038/ismej.2011.144

Sieber, M., Pita, L., Weiland-Bräuer, N., Dirksen, P., Wang, J., Mortzfeld, B., … Traulsen, A. (2019). Neutrality in the Metaorganism. *PLoS Biology*, *17*(6), e3000298. doi:10.1371/journal.pbio.3000298

Somoza, L., Rueda, J. L., González, F. J., Rincón-Tomás, B., Medialdea, T., Sánchez-Guillamón, O., … Reitner, J. (2021). A relict oasis of living deep-sea mussels Bathymodiolus and microbial-mediated seep carbonates at newly-discovered active cold seeps in the Gulf of Cádiz, NE Atlantic Ocean. *PalZ*, *95*(4), 793–807. doi:10.1007/s12542-021-00594-3

Song, H., Hewitt, O. H., & Degnan, S. M. (2020). Bacterial Symbionts in Animal Development: Arginine Biosynthesis Complementation Enables Larval Settlement in a Marine Sponge. SSRN Electronic Journal. doi:10.2139/ssrn.3664365

Stewart, F. J., Newton, I. L. G., & Cavanaugh, C. M. (2005). Chemosynthetic endosymbioses: adaptations to oxic–anoxic interfaces. Trends in Microbiology, 13(9), 439–448. doi:10.1016/j.tim.2005.07.007

Strathmann, R. R. (1985). Feeding and Nonfeeding Larval Development and Life-History Evolution in Marine Invertebrates. Annual Review of Ecology and Systematics, 16(1), 339–361. doi:10.1146/annurev.es.16.110185.002011

Thorson, G. (1950). Reproductive and Larval Ecology of Marine Bottom Invertebrates. Biological Reviews, 25(1), 1–45. doi:10.1111/j.1469-185x.1950.tb00585.x

Utermann, C., Parrot, D., Breusing, C., Stuckas, H., Staufenberger, T., Blümel, M., … Tasdemir, D. (2018). Combined genotyping, microbial diversity and metabolite profiling studies on farmed Mytilus spp. from Kiel Fjord. Scientific Reports, 8(1), 7983. doi:10.1038/s41598-018-26177-y

Wang, C., Sun, G., Li, S., Li, X., & Liu, Y. (2018). Intestinal microbiota of healthy and unhealthy Atlantic salmon Salmo salar L. in a recirculating aquaculture system. *Journal of Oceanology and Limnology*, *36*(2), 414–426. doi:10.1007/s00343-017-6203-5

Wentrup, C., Wendeberg, A., Schimak, M., Borowski, C., & Dubilier, N. (2014). Forever competent: deep-sea bivalves are colonized by their chemosynthetic symbionts throughout their lifetime. *Environmental Microbiology*, *16*(12), 3699–3713. doi:10.1111/1462-2920.12597

Wilkins, L. G. E., Leray, M., O'Dea, A., Yuen, B., Peixoto, R., Pereira, T. J., … Eisen, J. A. (2019). Host-associated microbiomes drive structure and function of marine ecosystems. PLOS Biology, 17(11), e3000533. doi:10.1371/journal.pbio.3000533

Young, C. M., Arellano, S. M., Hamel, J.-F., & Mercier, and A. (2017). Ecology and Evolution of Larval Dispersal in the Deep Sea (Vol. 1, pp. 1–22). Oxford University Press. doi:10.1093/oso/9780198786962.003.0016

Zhou, K., Zhang, R., Sun, J., Zhang, W., Tian, R.-M., Chen, C., … Xu, Y. (2019). Potential Interactions between Clade SUP05 Sulfur-Oxidizing Bacteria and Phages in Hydrothermal Vent Sponges. *Applied and Environmental Microbiology*, *85*(22). doi:10.1128/aem.00992-19

Zielinski, F.U., Pernthaler, A., Duperron, S., Raggi, L., Giere, O., Borowski, C., and Dubilier, N. "Widespread occurrence of an intranuclear bacterial parasite in vent and seep bathymodiolin mussels." Environ. Microbiol. (2009) 11:1150-1167.

Appendix A

Table 2A. Collection details, dive information, and sample IDs used during analysis.

Group	Sample ID	Submersible	Dive #	Altitude	Collection Method
Water	Niskin 3B	ROV Jason II	J2-1337	1.5 m	Niskin Bottle
Water	Niskin 3A	ROV Jason II	J2-1337	1.5 m	Niskin Bottle
Juvenile	MC 23	ROV Jason II	J2-1337	Bottom	Biobox
Juvenile	MC 22	ROV Jason II	J2-1337	Bottom	Biobox
Juvenile	MC 21	ROV Jason II	J2-1337	Bottom	Biobox
Juvenile	MC 20	Jason II	J2-1337	Bottom	Biobox
Juvenile	MC 19	Jason II	J2-1337	Bottom	Biobox
Pediveliger	MC 31	Jason II	J2-1337	Bottom	Biobox
Pediveliger	MC 30	Jason II	J2-1337	Bottom	Biobox
Pediveliger	MC 12	Jason II	J2-1337	Bottom	Biobox
Pediveliger	MC 11	Jason II	J2-1337	Bottom	Biobox
Pediveliger	MC 10	Jason II	J2-1337	Bottom	Biobox
Veliger	MC 16	AUV Sentry	S595P	5 m	SyPRID
Veliger	MC 15	AUV Sentry	S595P	5 m	SyPRID
Veliger	MC 08	AUV Sentry	S595P	5 m	SyPRID
Veliger	MC 07	AUV Sentry	S595P	5 m	SyPRID

Table 2B. Sequence ID's and bioinformatic processing information.

Group	Sequence ID	DNA conc. (ng/ul)	Raw Reads	Final Reads	Chimeric Reads	% Reads Retained	ASVs
Water	56230	7.84	27542	5907	132	0.214	344
Water	56229	8.48	56481	12216	414	0.216	394
Juvenile	56228	2.99	25682	15020	209	0.585	69
Juvenile	56227	1.56	21479	12907	48	0.601	34
Juvenile	56226	3.92	25449	12614	107	0.496	115
Juvenile	56225	2.14	15587	10242	6	0.657	52
Juvenile	56224	1.58	12843	8043	5	0.626	58
Pediveliger	56223	2.11	10816	5572	0	0.515	103
Pediveliger	56222	1.14	2282	991	0	0.434	45
Pediveliger	56221	1.42	2185	1307	0	0.598	34
Pediveliger	56220	0.749	16095	10451	0	0.649	42
Pediveliger	56219	0.776	10005	6367	3	0.636	35
Veliger	56218	0.843	11950	7161	0	0.59922	40
Veliger	56217	0.641	11998	7607	0	0.634	22
Veliger	56216	0.996	4376	2765	2	0.632	35
Veliger	56215	0.571	7636	4671	0	0.612	20

QIIME2 Pipeline for Analysis of V3/V4 16S rRNA sequences

STEP 1: IMPORT DATA

```
qiime tools import \
--type 'SampleData[PairedEndSequencesWithQuality]' \
--input-path /data/home/WWU/beavert2/magical_micro2 \
--input-format CasavaOneEightSingleLanePerSampleDirFmt \
--output-path demux-paired-end.qza
```

STEP 2: TRIM PRIMERS

```
qiime cutadapt trim-paired \
--i-demultiplexed-sequences demux-paired-end.qza \
--p-front-f CCTACGGGNGGCWGCAG \
--p-front-r GACTACHVGGGTATCTAATCC \
--p-error-rate 0 \
--o-trimmed-sequences trimmed.seqs.qza
```

STEP 3: JOIN/MERGE PAIRED-ENDS

```
qiime vsearch join-pairs \
--i-demultiplexed-seqs trimmed.seqs.qza \
--o-joined-sequences joined.seqs.qza \
--p-minovlen 20 \
--p-maxdiffs 10 \
--p-minmergelen 350 \
--p-maxmergelen 550 \
--p-allowmergestagger \
--p-truncqual 10 \
--p-minlen 100 \
--p-qmax 41 \
--p-qmaxout 41
```

STEP 4: QUALITY CONTROL PAIRED-END READS

```
qiime quality-filter q-score \
--i-demux joined.seqs.qza \
--o-filtered-sequences filtered.seqs.qza \
--o-filter-stats filter.stats.qza \
--p-quality-window 5 \
--p-min-quality 25
```

Visualization

```
qiime demux summarize \
--i-data filtered.seqs.qza \
--o-visualization filtered.seqs.qzv
```

STEP 6: DENOISE PROCESSED READS

```
qiime deblur denoise-16S \
--i-demultiplexed-seqs filtered.seqs.qza \
--p-trim-length 400 \
--o-representative-sequences deblur-rep.seqs.qza \
--o-table table.qza \
--p-sample-stats \
--o-stats deblur-stats.qza
```

EXAMINE READS POST DENOISING

```
qiime metadata tabulate \ --m-input-file deblur-stats.qza \ --o-visualization
deblur_stats.qzv qiime feature-table summarize \ --i-table filtered-table.qza
\ <-- filtered table has archaea removed, final read counts --o-visualization
table_vis.qzv \ --m-sample-metadata-file magical_metadata2.tsv qiime feature-
table tabulate-seqs \ --i-data deblur-rep.seqs.qza \ --o-visualization rep-
seqs-vis.qzv
```

STEP 7: CREATE PHYLOGENY

ALIGNMENT OF REPRESENTATIVE SEQUENCES

```
qiime alignment mafft \
--i-sequences deblur-rep.seqs.qza \
--o-alignment alignment.qza
```

MASK HIGHLY VARIABLE NOISY POSITIONS IN ALIGNMENT

```
qiime alignment mask \
--i-alignment alignment.qza \
--o-masked-alignment masked-alignment.qza
```

CREATE PHYLOGENY WITH FASTTREE (UNROOTED)

```
qiime phylogeny fasttree \
--i-alignment masked-alignment.qza \
--o-tree tree.qza
```

ROOT PHYLOGENY AT MIDPOINT

```
qiime phylogeny midpoint-root \
--i-tree tree.qza \
--o-rooted-tree rooted-tree.qza
```

STEP 8: ASSIGN TAXONOMY WITH TRAINED CLASSIFIER

```
qiime feature-classifier classify-sklearn \
--i-classifier silva-138-99-nb-classifier.qza \
--i-reads deblur-rep.seqs.qza \
--o-classification classification.qza \
--p-confidence 0.95 \
--p-read-orientation same
```

STEP 9: FILTER ARCHAEA

```
qiime taxa filter-table \
--i-table table.qza \
--i-taxonomy classification.qza \
--p-exclude Archaea \
--p-mode contains \
--o-filtered-table filtered-table.qza
```

STEP 10: RAREFY FEATURE TABLE

```
qiime feature-table rarefy \
  --i-table filtered-table.qza
  --p-sampling-depth 1179 \
  --p-with-replacement \
  --o-rarefied-table rarefied-table.qza
```

R-code for statistics and visualizations

```
library(ggplot2)
library(qiime2R)
library(phyloseq)
library(DEseq2)
library(vegan)
library(BiocManager)
library(knitr)
library(pairwiseAdonis)
library(devtools)
library(dendextend)
```

#convert QIIME .qza artifact to Phyloseq object, not rarefied!#

```
physeq<-qza_to_phyloseq(
  features="filtered-table.qza",
  tree="rooted-tree.qza",
  "classification.qza",
  metadata = "magical_metadata2.tsv")

#convert rarefied QIIME artifact to phyloseq object#
physeq.rare<-qza_to_phyloseq(
  features="rarefied-table.qza",
  tree="rooted-tree.qza",
  "classification.qza",
  metadata = "magical_metadata2.tsv")

# Library Size column
Libsize<-sample_sums(physeq)
sample_data(physeq)$Libsize <- Libsize

#Centered log ratio
x2 <- microbiome::transform(physeq, "clr")
summarize_phyloseq(x2)

#Variance stabilizing transformation
diagdds = phyloseq_to_deseq2(physeq, ~ group)
diagdds <- estimateSizeFactors(diagdds, type = "poscounts")
diagdds = estimateDispersions(diagdds)
diagvst = getVarianceStabilizedData(diagdds)
dim(diagvst)
physeq0 = physeq
otu_table(physeq) <- otu_table(diagvst, taxa_are_rows = TRUE)
physeq.vst<-physeq

#Scaled-ranked subsampling
Cmin = min(sample_sums(physeq))
#extract otu table and transpose
otus <- as.data.frame(otu_table(physeq))
#run SRS on otu table
SRS.otus <- SRS(otus, Cmin, set_seed = TRUE, seed = 1)
row.names(SRS.otus) <- row.names(otus)

#check if any OTUs were removed
SRS.otus[rowSums(SRS.otus) == 0,] #3 ASVs with 0 counts?

#make new ps object with the normalized otu table
ps.SRS <- physeq
otu_table(ps.SRS) <- otu_table(SRS.otus, taxa_are_rows = TRUE)
max(sample_sums(ps.SRS))

sample_data(ps.SRS)$Libsize <- Libsize

#Re-ordering samples
sample_data(physeq)$group<-factor(sample_data(physeq)$group, levels =
c("Juvenile","Pediveliger","Veliger"))
sample_data(physeq.vst)$group<-factor(sample_data(physeq.vst)$group, levels =
c("Niskin", "Juvenile","Veliger","Pediveliger"))

#Rarefaction curve
```

```
rarecurve(t(otu_table(physeq)), step=50, cex=0.5, label = FALSE, col =
sample_data(physeq)$group, ylab = "ASV's")

#Alpha diversity plot - Figure 3
plot_richness(physeq, x="group", measures = c("Observed"))

## Kruskal-wallis Test on Alpha Diversity
alphaObserved = estimate_richness(physeq0, measures="Observed")
 alpha.stats <- cbind(alphaObserved, sample_data(ps.SRS))
kruskal.test(alpha.stats$Observed, alpha.stats$group, data = alpha.stats)
pairwise.wilcox.test(alpha.stats$Observed, alpha.stats$group, p.adjust.method
= "BH")

# Calculate distance matrix
uunifrac <- phyloseq::distance(physeq.vst, method = "uunifrac")

#uunifrac <- phyloseq::distance(ps.SRS, method = "uunifrac")
#uunifrac <- phyloseq::distance(physeq.rare, method = "uunifrac")
#uunifrac <- phyloseq::distance(x2, method = "uunifrac")

# make a data frame from the sample_data
sampledf <- data.frame(sample_data(physeq.vst))
#sampledf <- data.frame(sample_data(physeq.rare))
#sampledf <- data.frame(sample_data(ps.SRS))
#sampledf <- data.frame(sample_data(x2))

# BETA DIVERSITY TEST #
## Permanova test on Beta Diversity
adonis2(uunifrac ~ group, data = sampledf)
#test effects of each normalization method on libsize and choose best one
adonis2(uunifrac ~ Libsize, data = sampledf)

#Pairwise adonis
pairwise.adonis2(uunifrac ~ group, data = sampledf)

#Hierarchical clustering - dendrogram
MM.tip.labels <- as(get_variable(physeq.vst, "group"), "character")
MM.hclust     <- hclust(uunifrac, method="average")
dend <- as.dendrogram(MM.hclust)
colors_to_use <- as.numeric(sample_data(physeq.vst)$group)
colors_to_use <-
numbers<-as.numeric(sample_data(physeq.vst)$group)
colors_to_use<-
c("#000000","#009E73","#000000","#56B4E9","#E69F00","#56B4E9","#000000","#E69
F00","#56B4E9","#009E73","#009E73","#000000","#000000","#009E73","#56B4E9","#
009E73")

colors_to_use <- colors_to_use[order.dendrogram(dend)]
colors_to_use
labels_colors(dend) <- colors_to_use
    # change labels
labels(dend) <- c("Niskin","Niskin",
"Juvenile","Juvenile","Juvenile","Juvenile","Juvenile","Veliger","Veliger","V
eliger","Veliger","Pediveliger","Pediveliger","Pediveliger","Pediveliger","Pe
diveliger")

dend# Patient labels have a color based on their group
```

```
labels_colors(dend)
plot(dend, main = "Hierarchical Clustering", xlab="Group")

dend %>% set("leaves_col", 1) %>% # adjust the leaves
  hang.dendrogram %>% # hang the leaves
  plot(main = "Hierarchical Cluster Analysis")
```

 # Relative abundance stacked barplot

#Pruning niskin samples

```
sample_data(physeq)
to_remove <- c("56229", "56230")

noniskin_physeq <- prune_samples(!(sample_names(physeq) %in% to_remove),
physeq)
sample_data(noniskin_physeq)
```

Sorting top 50 ASV's

```
topN = 50
most_abundant_taxa = sort(taxa_sums(z), TRUE)[1:topN]
print(most_abundant_taxa)
physeq_t50 = prune_taxa(names(most_abundant_taxa), z)
otu_table(physeq_t50)

physeq_relabund = transform_sample_counts(physeq_t50, function(x) x / sum(x)
)
otu_table(physeq_relabund)
```

Order level

```
glom <- tax_glom(physeq_relabund, taxrank = 'Order')

glom # should list # taxa as # Class or Family
data_glom<- psmelt(glom) # create dataframe from phyloseq object

data_glom$Order <- as.character(data_glom$Order) #convert to character

data_glom$Order[data_glom$Abundance < 0.01] <- "< 1% abund."

data_glom[data_glom==0] <- NA

Count = length(unique(data_glom$Order))
unique(data_glom$Order)

data_glom$Order <- factor(data_glom$Order, levels = c("Methylococcales",
                                                      "Pseudomonadales",
                                                      "Sphingomonadales",
                                                      "Alteromonadales",
                                                      "Nitrosococcales",
                                                      "Burkholderiales",
                                                      "Thiomicrospirales",
                                                      "Thiotrichales",
                                                      "Oceanospirillales",
                                                      "Cytophagales",
                                                      "Vibrionales",
                                                      "Campylobacterales",
                                                      "Chloroplast",
                                                      "Verrucomicrobiae",
```

```
                                                    "Bacillales",
                                                    "< 1% abund."))

#Order level
spatial_plot <- ggplot(data=data_glom, aes(x=individual,y=Abundance,
fill=Order)) + facet_grid(~group, scales = "free")
## Trying to re-order groups
spatial_plot$data$group<-factor(spatial_plot$data$group,
levels=c("Juvenile","Pediveliger","Veliger"))
spatial_plot + geom_bar(aes(), stat="identity", position="stack") +
  scale_fill_manual(values = col_vector) +
  theme(legend.position="bottom") + guides(fill=guide_legend(nrow=4)) +
  theme(axis.title.x=element_blank(),
        axis.text.x=element_blank(),
        axis.ticks.x=element_blank())

col_vector<- c("#7FC97F", "#BEAED4", "#FDC086", "#FFFF99", "#386CB0",
"#F0027F", "#BF5B17", "skyblue2", "#1B9E77", "#D95F02",
"#7570B3", "gold1", "#66A61E", "black", "#A6761D",
"gray70", "#A6CEE3", "#1F78B4", "#E31A1C")

#Heatmap
myranks = c("Family","Genus","Species")
order<-c("56228","56227","56226","56225","56224","56223","56222","56221",
"56220","56219","56218","56217","56216", "56215","56230","56229")

plot_heatmap (physeq_relabund, taxa.label=myranks,
         taxa.order="Phylum", low="royalblue2", high="magenta", na.value =
         "black", sample.order=order, sample.label="group")
```